Biochimica et Biophysica Acta 857 (1986) 85–94
Elsevier

BBA 73055

The microsecond rotational motions of eosin-labelled fatty acids in multilamellar vesicles

Edward Blatt * and Alan F. Corin **

Abteilung Molekulare Biologie, Max-Planck-Institut für Biophysikalische Chemie, Postfach 2841, D-3400 Göttingen (F.R.G.)

(Received August 30th, 1985)
(Revised manuscript received January 8th, 1986)

Key words: Rotational motion; Multilamellar vesicle; Phosphorescence anisotropy; Eosin; Luminescence quenching

The rotational properties of two eosin-labelled fatty acids of different alkyl chain length have been studied in large multilamellar dimyristoylphosphatidylcholine vesicles. The location of the probes at the surface region were ascertained by quenching experiments using a hydrophilic divalent cation solubilized in the aqueous phase (Cu^{2+}) and a hydrophobic aromatic aniline (*N*,*N*-dimethylaniline) associated with the lipid. Phosphorescence anisotropy measurements reveal that above the phospholipid phase transition the polarization of eosin luminescence decays monoexponentially in the micro-to-millisecond time range, while below the phase transition a biexponential decay is observed. A model is proposed which attributes the time constants to two separate motions, discrete jumps or 'flipping' of the eosin moiety within restricted boundaries and long-axis rotation. The value of the time-independent term changes with probe position and temperature and reflects orientational constraints imposed by lipid-chromophore interactions. The implications of these results for the study of protein rotations in membranes are discussed.

Introduction

The rotational diffusion of proteins reconstituted into membranes or as integral cell components occurs typically in the microsecond-to-millisecond time domain [1–4]. Phosphorescence anisotropy techniques, exploiting extrinsic luminescent probes, provide a suitable means of studying these motions as the triplet lifetimes of a number of chromophores are in the same time region [5]. An important assumption underlying the method, however, is that independent motions of the probe which depolarize the emission can be excluded over the time range of protein rotation. This assumption is of particular importance in the case of eosin-labelled proteins, where multiple phosphorescence lifetimes and rotational correlation times are often observed [6,7].

In order to address this problem specifically, and to obtain information on lipid dynamics and structure, the rotational motions of two eosin fatty-acid probes, 4-(*N*-dodecanoyl)amidoeosin and 4-(*N*-hexadecanoyl)amidoeosin (Scheme I, $n = 11$ and 15, respectively), were observed in large multilamellar dimyristoylphosphatidylcholine (DMPC) vesicles over a range of temperatures. The location of the probes in the bilayer was

* Present address: CSIRO Division of Applied Organic Chemistry, G.P.O. Box 4331, Melbourne, Vic. 3001, Australia.

** To whom correspondence should be addressed at (present address): Kodak Research Laboratories, Life Sciences Division, Rochester, NY 14650, U.S.A..

Abbreviations: E12, 4-(*N*-dodecanoyl)amidoeosin; E16, 4-(*N*-hexadecanoyl)amidoeosin; DMPC, dimyristoylphosphatidylcholine; EITC, eosin 5'-isothiocyanate.

0005-2736/86/$03.50 © 1986 Elsevier Science Publishers B.V. (Biomedical Division)

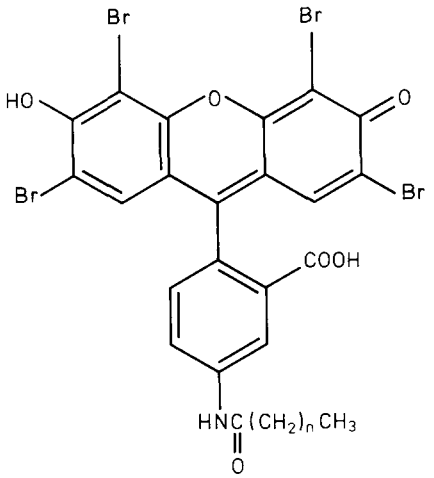

Scheme I. Eosin-labelled fatty acids.

assessed by quenching measurements using the water-soluble quencher Cu^{2+} and the hydrophobic quencher, *N,N*-dimethylaniline. The phosphorescence emission from the eosin chromophores depolarized in the microsecond time domain to a constant residual anisotropy. A model is proposed in which the degree of the angular constraints of rotation is indicative of the extent to which the eosin moiety is buried in the bilayer.

Materials and Methods

4-(*N*-Dodecanoyl)amidoeoson (E12), 4-(*N*-hexadecanoyl)amidoeosin (E16) and eosin 5′-isothiocyanate (EITC) were purchased from Molecular Probes. Incorporation of the former two probes into large multilamellar DMPC vesicles (Sigma) was achieved by adding 9 μl of a 1 mg/ml methanol solution of probe to 15 mg of DMPC dissolved in 2 ml of a 2 : 1 mixture of chloroform/methanol. In this manner, a lipid-to-probe ratio of 2000 : 1 was obtained. The solvent was removed by rotary evaporation. Subsequently, 2 ml of a 10 mM phosphate buffer (pH 7.0) was added and the flask was brought to 30°C and gently swirled. The resulting suspension was washed three times by centrifugation at 12 500 × *g* in an Eppendorf table-top centrifuge (model 5412) for 1.5 min, this being followed by careful removal of the clear supernatant with a pipette and resuspension of the vesicles in 2 ml buffer. The bright pink pellet seen after centrifugation established the incorporation of the probes into the multilayer structures. $CuSO_4$ (Merck) and *N,N*-dimethylaniline (EGA, > 99% pure) were used as provided.

Measurements of phosphorescence depolarization were made with an instrument previously described [43,44]. The parallel, $I_{\parallel}(t)$, and perpendicular, $I_{\perp}(t)$ components of emission were collected and arranged to generate the total time-dependent emission $S(t) = I_{\parallel}(t) + 2I_{\perp}(t)$ and time-dependent anisotropy $r(t) = [I_{\parallel}(t) - I_{\perp}(t)]/S(t)$. Decay profiles were then fitted by a least-squares iterative procedure with up to three exponential terms and a constant. The fits chosen to represent the data were decided by inspection of the residuals plots; if inclusion of additional terms did not improve the randomness of the residuals, the fit with less terms was maintained. Steady-state fluorescence intensities were measured on an SLM 8000/8000S Spectrofluorimeter using an excitation wavelength of 520 nm and observing the emission at 600 nm.

Quenching experiments with Cu^{2+} and dimethylaniline were carried out at 26°C and 22°C, respectively, by addition of small aliquots of the appropriate stock solutions: 10 mM phosphate buffer (pH 7.0) for Cu^{2+} and methanol for dimethylaniline. In order to ensure incorporation of quencher into the aqueous phases of the multilayered vesicles, the samples were repeatedly heated and cooled through the phase-transition temperature after each aliquot and finally allowed to equilibrate for 30 min. In the case of phosphorescence lifetime measurements, oxygen was removed by passing a continuous stream of high purity argon gas (Messer Griesheim, 99.998% pure) over the solution in the cuvette while gently stirring with an overhead motor-driven propeller blade. The effects of light scattering were minimized by use of low vesicle concentrations, typically 200 μM in DMPC.

Estimation of size and extent of fatty-acid incorporation into the multilamellar vesicles were assessed by viewing a labelled sample in a Zeiss Universal fluorescence microscope with a television camera. The relative fluorescence intensity in the vesicles and in the bulk aqueous phase was determined with the use of image analysis procedures. The vesicles were found to be fairly uni-

form in size and sphericity, with a diameter of 5.8 ± 0.6 μm. No fluorescence could be detected from the aqueous phase, indicating negligible partitioning of the eosin fatty acids from the lipid phase into the aqueous phase.

Results

Cu^{2+} quenching

Cu^{2+} has previously been shown to quench the emission of a number of fluorescent probes in DMPC liposomes [8] and anionic surfactant micelles [9,10], as well as the phosphorescence of triplet probes [11,12]. In the former set of experiments, quenching efficiencies for a series of probes were interpreted in terms of chromophore location. A similar strategy was used here to assess the positions of the eosin fatty acids in the bilayer.

Fig. 1a shows the change in the total phosphorescent emission of E16 in DMPC vesicles with added Cu^{2+} and Fig. 1b shows Stern-Volmer plots [13] under a number of conditions. Addition of quencher did not change the anisotropy characteristics. Phosphorescent lifetimes (τ) were generally adequately described by single exponential functions in buffer. However, higher-order fits were necessary when probes were examined in vesicles: in this case, average lifetimes ($\langle\tau\rangle = \sum_{i=1}^{3}\alpha_{\tau i}$, where α_i are the fractional amplitudes) were used to generate the plots [14,15].

A number of interesting points arise from the data presented. In buffer at 20°C, values of τ for E12 and E16 were 829 and 825 μs, respectively, somewhat higher than 502 μs for EITC. Upon incorporation into the vesicles, the average lifetimes increased to 1725 and 1081 μs for E12 and E16, respectively, indicating the effects of different solubilization sites. This interpretation is substantiated by consideration of the following features of Fig. 1b. First, the degree of quenching is similar for both probes in buffer. In DMPC, the E12 derivative is quenched more than the E16 derivative. As the association of divalent cations to phosphatidylcholine is very weak [16], we might expect Cu^{2+} ions to locate mainly in the aqueous phase. Thus the eosin moiety of the E12 derivative is more accessible to Cu^{2+} ions associated with the lipid/water interface than E16. Recent phosphorescence-quenching measurements indicate that erythrosin is also localized in the polar surface region of liposome membranes [17].

The second feature of Fig. 1b is an observed plateau as the concentration of quencher increases. In macrostructures, this could arise as the

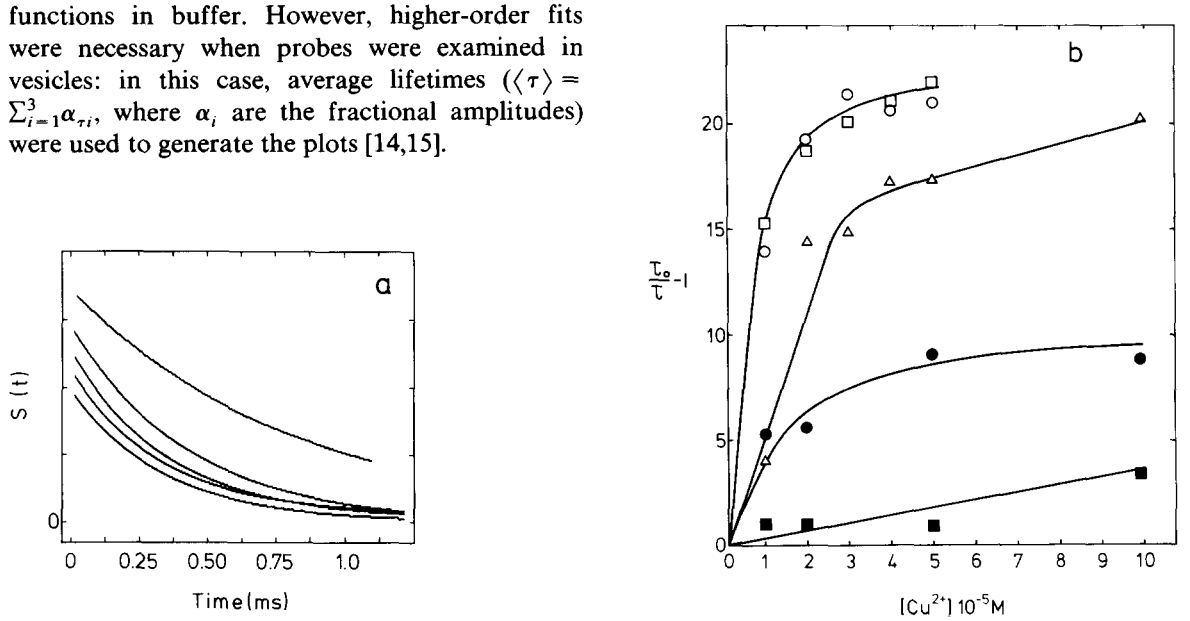

Fig. 1. (a) Fitted phosphorescence emission profiles of E16 in DMPC vesicles with increasing Cu^{2+}: at early times from top to bottom $Cu^{2+} = 0$, 10^{-5}, $2\cdot10^{-5}$, $5\cdot10^{-5}$, 10^{-4} M. $S(t)$ is the time-dependent total phosphorescence emission. (b) Stern-Volmer plots for the quenching by Cu^{2+} of the phosphorescence lifetimes of E12 and E16 in buffer (○, □) and DMPC vesicles (●, ■), respectively, and EITC in buffer (△), at 26°C. The Stern-Volmer term ($\tau_0/\tau - 1$) of Eqn. 1 is explained in the text. Solid lines are drawn for clarity and are not the result of any fitting procedure.

result of: (i) a proportion of chromophores not being accessible to the quencher [18]; (ii) two populations of accessible chromophores [19]: (iii) the total concentration of quencher being used on the abscissa rather than the bound quencher [8]. However, since similar Stern-Volmer plots are obtained in buffer, these three explanations can not completely account for the data. The low probe concentrations used and the plateau effect for EITC rule out the possibility of micelle formation in the case of the fatty-acid probes. Instead, the data may be interpreted by consideration of the following process [14]:

$$A^* + Q \underset{k_{-d}}{\overset{k_d}{\rightleftharpoons}} (A^* \ldots Q) \overset{k_i}{\rightarrow} A + Q + \text{heat}$$

where A* and Q are the excited state chromophore and quencher, respectively, k_d and k_{-d} are the diffusion-limited rate constants for formation and breakdown of an encounter complex (A*...Q), respectively, and k_i is the rate constant for the non-radiative deactivation of the electronically excited state in the encounter complex. The Stern-Volmer equation then becomes

$$(\tau_0/\tau) - 1 = k_q \tau_0 [Q] \quad (1)$$

where τ_0 is the phosphorescence lifetime in the absence of quencher ($\tau_0 = \langle \tau_0 \rangle$ in the case of multiple exponential decay) and k_q is the apparent rate constant for quenching equal to γk_d, where

$$\gamma = k_i / (k_i + k_{-d} + \tau_0^{-1} + k_d[Q]) \quad (2)$$

Eqn. 2 predicts a value of γ less than 1 when k_i is of the same magnitude or is lower than the other rate constants, and plateauing of Stern-Volmer plots when $k_d[Q]$ is significant. As k_{-d} can be significantly lower than k_d for excited state complexes [20], $k_d[Q]$ may become comparable to k_i, and k_q is a function of [Q]. The quenching of triplet states by ions of the first transition series does involve the formation of a collision complex followed by an energy transfer process. The rate constants for this process are approximately $5 \cdot 10^7$ $M^{-1} \cdot s^{-1}$ [11], which is two orders of magnitude less than that expected for a diffusion controlled reaction. Initial slopes of the Stern-Volmer plots in buffer (Fig. 1b) also give rate constants of similar magnitude ($k_q \approx 10^8$ $M^{-1} \cdot s^{-1}$). Thus, it seems likely that Cu^{2+} quenching of the triplet states of eosin and its derivatives proceeds by an energy-transfer process involving charge-transfer complexes.

Dimethylaniline quenching

Dimethylaniline is a hydrophobic molecule which shows a high affinity for the lipid phases of bilayer vesicles and surfactant micelles [21]. Its ability to quench membrane-associated lumophores is thus expected to be greater than that of Cu^{2+}. Indeed, comparable concentrations of dimethylaniline resulted in complete quenching of the phosphorescence emission of the two eosin fatty-acid probes on the microsecond time scale. As the fluorescence lifetime of eosin in a number of solvents is in the order of a few nanoseconds [22], it was envisaged that fluorescence-quenching measurements would be more appropriate.

Fig. 2 shows the steady-state Stern-Volmer plots obtained. In contrast to the Cu^{2+} quenching data, the quenching efficiency of E16 was greater than

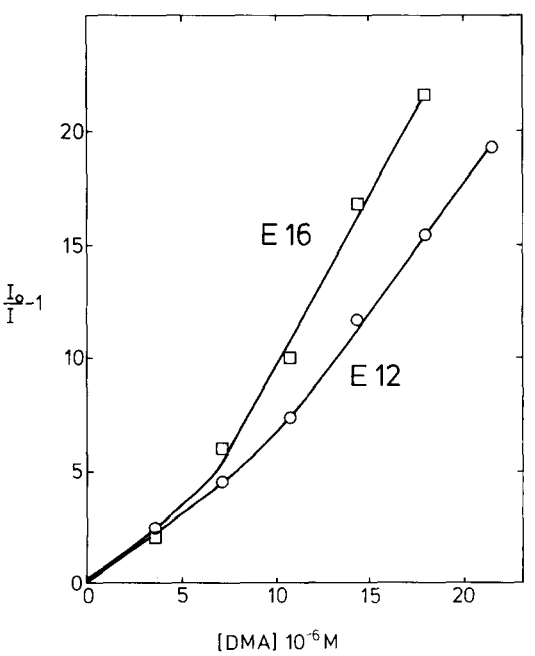

Fig. 2. Stern-Volmer plots for the quenching of the steady-state fluorescence of E12 and E16 by DMA and DMPC vesicles at 22°C. I_0 and I are the fluorescence intensities in the absence and presence of quencher, respectively.

that of E12. If the fluorescence lifetimes of E12 and E16 are proportional to the steady-state emission intensities (approx. 1.4 : 1.0, respectively), the relative quenching efficiencies become more disparate. As dimethylaniline preferentially locates near the centre of the bilayer [8], the data infer that E12 locates closer to the bulk aqueous phase than E16, in agreement with the interpretation of the Cu^{2+}-quenching measurements. The upward curvatures observed are probably, due to a significant contribution of static quenching [8–10].

Phosphorescence lifetime and anisotropy measurements in DMPC vesicles

Having established the incorporation and relative location of the two eosin fatty acids in the bilayer, the dependence of phosphorescent lifetimes and anisotropies on temperature were assessed. The decays of the total emission were best fit by a sum of three exponentials. Fig. 3 shows the dependence of $\langle\tau\rangle$ as a function of temperature. In both cases an abrupt decrease is observed as the temperature is raised through the upper transition temperature of the multilamellar DMPC vesicles ($T_t \approx 23$°C [23,24]). (Analogous correlations between average lifetimes and lipid structure have also been observed using the fluorescence characteristics of 1,6-diphenyl-1,3,5-hexatriene in membranes [25] and a series of *n*-(9-anthroyloxy) fatty acids in bilayer vesicles [26].) The emission properties of eosin are very sensitive to solvent composition, e.g., the phosphorescent lifetimes for E12 in butanol and acetonitrile at 20°C were 486 and 70 μs, respectively (data not shown). Thus the different lifetimes of the two probes in the vesicle, and the large dependence of $\langle\tau\rangle$ as the temperature is raised, reflect different chromophore location and dynamic interactions with the bilayer.

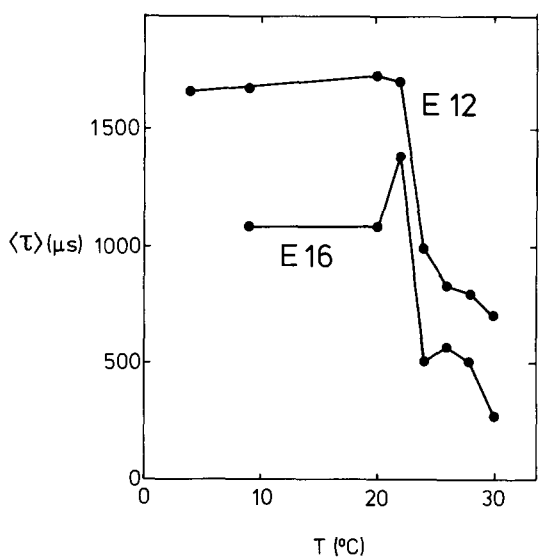

Fig. 3. The dependence of the average phosphorescent lifetimes $\langle\tau\rangle$ of E12 and E16 in DMPC vesicles with temperature.

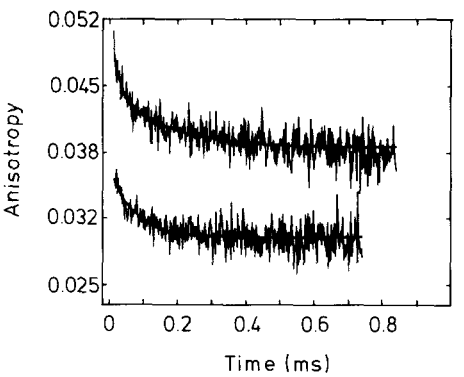

Fig. 4. Anisotropy profiles and lines of best fits (superimposed smooth curves) for E12 in DMPC vesicles at 10°C (upper curve) and 30°C (lower curve). See Table I and Fig. 5 for fitted parameters.

Typical anisotropy decays in DMPC vesicles are shown in Fig. 4. In buffer, the $r(t)$ profiles were centered about 0. Parameters describing the curves were obtained by fitting the profiles to an equation of the form

$$r(t) = (r_0 - r_\infty)\sum_{i=1}^{2}\beta_i \exp(-t/\phi_i) + r_\infty \qquad (3)$$

where r_0 and r_∞ are the initial and residual anisotropies, respectively, ϕ_i are the rotational correlation times and β_i are the corresponding fractional amplitudes. Table I lists the fitted anisotropy parameters obtained for E12 and E16, and Fig. 5 shows graphically the dependence of r_∞ and rotational correlation times as a function of temperature. (Values of r_8 are given in Table I due to the uncertain effects on the photomultiplier gain recovery after gating of the high intensity prompt fluorescence at early times.) For both fatty-acid probes, anisotropy decays above T_t were described by single exponential functions with correlation

TABLE I

ROTATIONAL CORRELATION PARAMETERS FOR E12 AND E16 IN MULTILAMELLAR DMPC VESICLES AS A FUNCTION OF TEMPERATURE

Correlation times ϕ_i are given in μs and β_i are fractional amplitudes extrapolated to time zero. r_8 is the anisotropy at time $t = 8$ μs, explained in text.

Temp. (°C)	E12						E16					
	β_1	ϕ_1	β_2	ϕ_2	r_8	r_∞	β_1	ϕ_1	β_2	ϕ_2	r_8	r_∞
30	1.0	62	–	–	0.036	0.030	1.0	50	–	–	0.036	0.029
28	1.0	48	–	–	0.038	0.032	1.0	57	–	–	0.038	0.032
26	1.0	64	–	–	0.036	0.030	1.0	68	–	–	0.036	0.031
24	1.0	48	–	–	0.036	0.030	1.0	47	–	–	0.038	0.032
22	0.77	34	0.23	364	0.039	0.031	0.46	19	0.54	124	0.052	0.037
20	0.69	30	0.31	392	0.043	0.032	0.49	34	0.51	211	0.050	0.037
10	0.55	17	0.45	265	0.049	0.039	0.75	16	0.25	128	0.062	0.051
2	0.76	19	0.24	283	0.054	0.042						

times, ϕ, of about 55 μs, while two exponentials (ϕ_1, ϕ_2) were necessary below T_t, where $\phi_1 < \phi < \phi_2$. Addition of Cu^{2+} did not change the fitted anisotropy parameters listed in Table I.

Discussion

Luminescence studies of fluorescent probes incorporated in bilayers have reported rotational motions in the nanosecond time domain, reflecting the diffusive properties of lipid molecules. The microsecond rotations observed here are, we believe, to be the first of their kind in this time domain. In order to interpret the data, two trivial sources of long relaxation times warrant consideration, namely, vesicle rotation and lateral diffusion of the eosin chromophore around the surface of the vesicle. In the former case, a vesicle with a radius of about $2.9 \cdot 10^{-6}$ m would have a rotational correlation time in the vicinity of 30 s, thus

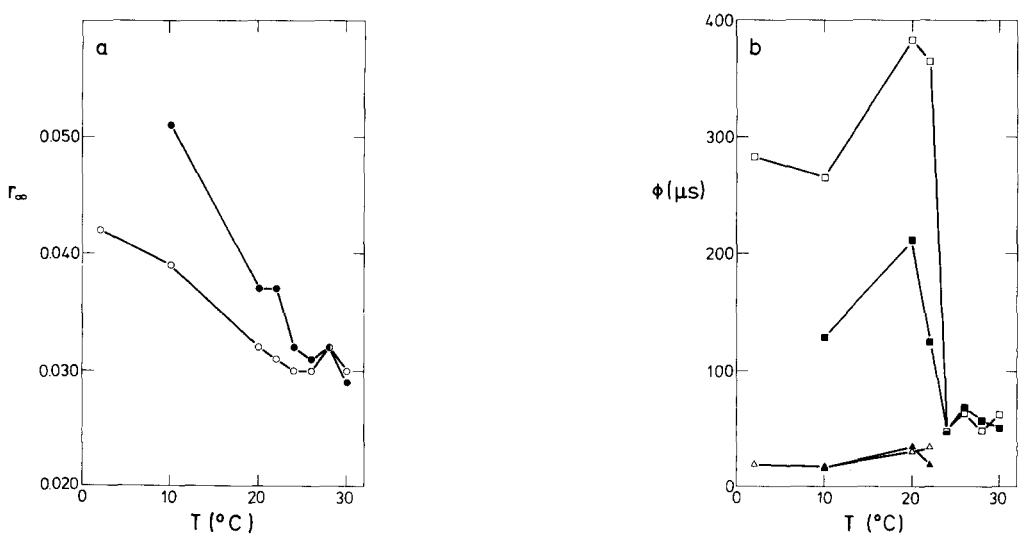

Fig. 5. The dependence of (a) the residual anisotropy (r_∞), and (b) the rotational correlation times (ϕ), for E12 (open symbols) and E16 (filled symbols) in DMPC vesicles as a function of temperature. Above T_t, the correlation times observed were attributed to discrete jumps of the probes (□), while below T_t second components appeared which were attributed to long-axis rotation (△). (See Discussion for details of data interpretation.)

providing a negligible contribution to the anisotropy decay. With respect to latteral diffusion, it has been shown that, in the absence of other depolarizing motions, a probe located on the surface of a spherical vesicle would have to move across a 40° arc for $r(t)$ to decay to $1/e$ of its original value [27,28]. This corresponds to a mean displacement of about $2 \cdot 10^{-6}$ m. Assuming a lateral diffusion coefficient of the fatty acid of between $4 \cdot 10^{-11}$ and $1 \cdot 10^{-7}$ $cm^2 \cdot s^{-1}$ [29], the time required for such a displacement can be obtained by substitution into Fick's law; this gives $t = 0.1$ s to 250 s, respectively, again outside the time range in this study.

A further possibility exists with respect to lateral diffusion. Here, the fatty acids can be envisaged as diffusing laterally around the perimeter of convolutions in the vesicle surface. As a first approximation, these surfaces are assumed to consist of a series of semispherical 'hills and valleys' with an average radius of curvature for each of $\langle r \rangle$. From fluorescence recovery after photobleaching experiments [29], the lateral diffusion coefficient in DMPC multibilayers of a probe similar to the fatty-acid derivatives used in this study (5-(hexadecanoylamino)fluorescein), was determined as $D = 10^{-7} cm^2 \cdot s^{-1}$ at 33°C. Substitution of D and $\phi = 55$ μs for the fatty-acid probes above T_t into Fick's law gives a mean displacement of $X = 470$ Å around the convoluted surface for the eosin chromophores. This value corresponds to $\langle r \rangle =$ 670 Å; the multilamellar vesicles used here have a radius of 58000 Å. For comparison, a sonicated unilamellar vesicle exhibits a typical radius of 100 Å [30]. At $T \approx 3$°C, the lateral diffusion for the fluorescein analogue displays one component with $D \approx 4 \cdot 10^{-11}$ $cm^2 \cdot s^{-1}$ [29]. Substitution of this value and $\phi_1 = 19$ μs or $\phi_2 = 283$ μs for the E12 derivative at $T = 2$°C into Fick's law, gives $X = 6$ Å and 21 Å, respectively, corresponding to $\langle r \rangle = 9$ Å and 30 Å. As a single phospholipid in a bilayer occupies an area of approx. 60 $Å^2$ [31], the above values of X and $\langle r \rangle$ are physically unrealistic. Hence, although the results above T_t are compatible with the notion of convoluted surfaces, the data below T_t rule out the possibility as a means of explaining the microsecond correlation times.

Single and double exponential decays are observed above and below T_t, respectively. An analogy can be drawn to the $r(t)$ curves that have been observed on the nanosecond time-scale for diphenylhexatriene [32–34] and a series of fatty acids [28] in DMPC vesicles. In the latter study, the results below T_t were interpreted in terms of microheterogeneity of solubilization sites. That is, values of ϕ_1 and ϕ_2 correspond to the rotational motions of two separate populations of fluorophores, while values of β_1 and β_2 represented the fractional contributions of each population, respectively. Both ϕ_1 and ϕ_2 were larger than the single value of ϕ above T_t. In contrast, the results presented here show that $\phi_1 < \phi < \phi_2$.

With the above factors in mind, we propose a model that incorporates the following experimental results: (1) the microsecond rotational correlation times: (2) the change in the number of exponentials required to fit the anisotropy data above and below T_t: (3) the independence of the anisotropy characteristics with added Cu^{2+}, indicating the uncoupled nature of $S(t)$ with $r(t)$): (4) the difference in values of r_∞ between the two probes: (5) the low values of r at early times (i.e., r_8) as compared to that expected for an immobilized eosin chromophore.

To begin, we refer to a recent electron spin resonance (ESR) study on molecular motions in phospholipid bilayers using fatty-acid spin labels [35]. In that study rotational correlation times of 60 to 100 μs were calculated for a phospholipid spin-label incorporated into DMPC bilayers between 5 and 15°C, and were attributed to long-axis rotation of the lipid molecules. Above T_t, correlation times in the order of nanoseconds were observed. In the light of these results, we consider that the shorter correlation times (ϕ_1) primarily reflect long-axis rotation of the probe below T_t. (These motions are not seen above T_t, as our phosphorescence spectrometer cannot measure emission processes in the submicrosecond range.) The slightly lower values of ϕ_1 compared with those obtained from the ESR studies probably reflect different chromophore size, structure and probe-lipid interaction. The longer correlation times below T_t (ϕ_2) and the single correlation time above T_t arise from discrete jumps or 'flipping' motions of the aromatic chromophore on the surface of the bilayer. The sharp decrease in correlation time observed as the temperature is raised

through the phase transition (Fig. 5b) is typical of dynamic measurements of probes in lipid bilayers [8,24,25,32–35]. The nature of the 'flipping' motion will be discussed after further examination of the anisotropy data.

A number of theoretical approaches have shown that the persistence of a nonzero anisotropy in membranes is indicative of hindered rotational motions of the chromophore [36–39]. That is, values of the ratio r_∞/r_0 provide information on the orientational constraints imposed by neighbouring molecules. Generally, larger values of r_∞/r_0 indicate greater constraints and narrower angular excursions of the probe [39]. Experimentally, values of r_0 may be determined by immobilizing the luminescent molecule either in glycerol at low temperatures or in polymer matrices such as polymethylmethacrylate. This procedure is of particular importance in phosphorescence anisotropy measurements as rotations in the submicrosecond time domain reduce initial observed anisotropies. The long-lived excited states of triplet probes allow accurate estimations of r_∞, especially when lifetimes are much greater than correlation times.

In order to interpret the anisotropy data shown in Fig. 5 the fundamental anisotropy, r_0, is assumed to be the same for the two probes over the temperature range studied. Our instrument gave $r_0 = 0.2$ for eosin in polymethylmethacrylate that was invariant with temperature (data not shown). Values of r_8 then reflect initial depolarizations brought about by rotational motions within the 8 μs deadtime of the instrument, e.g., long-axis rotation, although other processes must also contribute since depolarizations occur below T_t. Fig. 6 is a diagrammatic representation of the proposed locations of the probes in the bilayer. The eosin moiety of the E12 derivative is more removed from the ordered head-group region than in the case of the E16 derivative, allowing greater freedom of rotation. The deeper burial of the E16 derivative is expected due to the greater hydrophobicity of longer alkyl chains [40]. Above T_t, discrete jumps or flipping within limited boundaries occur, with rotational correlation times in the order of 55 μs for both probes. As the temperature is lowered below T_t, large increases in the correlation times occur. Simultaneously, a

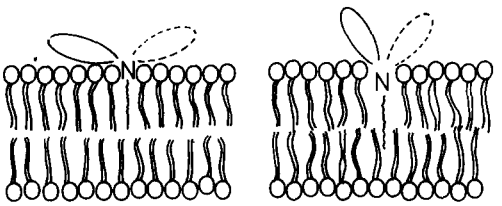

Fig. 6. Idealized schematic representation of the orientations of E12 (left) and E16 (right) in multilamellar DMPC vesicles. The oblong structures above the nitrogen atoms represent the eosin moiety. The solid and broken lines indicate the geometric boundaries of the restricted eosin rotation. Although the carbon chains for both eosin fatty acids are not drawn accurately to scale, E16 is shown as being longer than the E12. The interdigitation of the E16 chain with the opposing monolayer is a consequence of the representation; it has not been addressed experimentally in this work.

hitherto undetected second correlation time (ϕ_1) is resolved, the aforementioned long-axis rotation. The steady increase in values of r_∞ with decreasing temperature (Fig. 5a) reflects the smaller angular excursions of the chromophore. This is certainly, in part, due to lipid chain ordering [41], although changes in probe location (e.g., solubilization further into the bilayer) may be a contributing factor.

In conclusion, the appearance of correlation times in the microsecond time range for both eosin fatty acid probes, above (ϕ) and below (ϕ_1 and ϕ_2) the phase transition temperature, suggest rather 'long-lived' lipid head-group–eosin chromophore interactions. In accord with the model discussed above, the eosin can be seen as associating with one or more lipid head groups at the periphery of its motion. If the association step is diffusion-controlled (i.e., $k_{diff} > 10^9\ M^{-1} \cdot s^{-1}$) then the residence time (the reciprocal of the dissociation rate) defines the slow correlation times associated with the flipping motions. Regardless of the model chosen, the microsecond times observed in these experiments have significant implications in the interpretation of time-dependent anisotropy experiments of membrane proteins labelled with extrinsic triplet probes, measurements which also view motions in the microsecond time range. It is clear that under certain circumstances significant interaction between the chromophore and the lipid matrix will occur. As has been previously pointed out [42], this situation

may be advantageous when information on the mobility of membrane components is desired. However, in cases where knowledge of the rotational motion of a labelled protein incorporated in a membrane is sought, such interactions can yield data which are misleading. This problem may be circumvented by labelling of specific protected sites. For example, in a recent study, the galactoside-binding site in the lactose permease membrane protein of *Escherichia coli* was labelled with a fluorescent probe, shown to be located within the molecule [15]. That is, the binding site was inside the protein with respect to the lipid phase and with respect to the aqueous phase, ensuring that correlation times observed are not due to probe-membrane interactions. Such labelling of the lactose permease with eosin and location of the probe inside the protein have also been performed. The phosphorescence anisotropy characteristics have been examined in this laboratory by one of us (A.F.C.), in collaboration with K. Dormair and F. Jähnig, and will be reported elsewhere.

Acknowledgements

E.B. was supported by a stipendium from the Alexander-von-Humboldt Stiftung and A.F.C. by a Max Planck Gesellschaft Stipendium. We thank Dr. T.M. Jovin for his generous support, Dr. D. Marsh for reading and commenting on the manuscript and Dr. E. Matayoshi for his initial instructive contribution. We also thank Dr. M. Robert-Nicoud for conducting the fluorescence microscope measurements.

References

1 Edidin, M. (1974) Annu. Rev. Biophys. Bioeng. 3, 179–201
2 Cherry, R.J. (1976) Methods Enzymology 4, 47–61
3 Jovin, T.M., Bartholdi, M., Vaz, W.L.C. and Austin, R.H. (1981) Ann. NY Acad. Sci. 336, 176–196
4 Hoogevest, P., De Kruijff, B. and Garland, P.B. (1985) Biochim. Biophys. Acta 813, 1–9
5 Johnson, P. and Garland, P.B. (1982) Biochem. J. 203, 313–321
6 Austin, R.H., Chan, S.S. and Jovin, T.M. (1979) Proc. Natl. Acad. Sci. USA 76, 5650–5654
7 Eads, T.M., Thomas, D.D. and Austin, R.H. (1984) J. Mol. Biol. 179, 55–81
8 Thulborn, K.R. and Sawyer, W.H. (1978) Biochim. Biophys. Acta 511, 125–140
9 Blatt, E., Ghiggino, K.P. and Sawyer, W.H. (1981) J. Chem. Soc. Faraday Trans. I 77, 2551–2558
10 Blatt, E., Sawyer, W.H. and Ghiggino, K.P. (1984) J. Phys. Chem. 88, 3918–3920
11 Porter, G. and Wright, M.R. (1959) Disc. Faraday Soc. 27, 18–27
12 Kalyanasundaram, F.G., Grieser, F. and Thomas, J.K. (1977) Chem. Phys. Lett. 51, 501–505
13 Stern, V.O. and Volmer, M. (1919) Phys. Z. 20, 183–189
14 Eftink, M.R. and Ghiron, C.A. (1981) Anal. Biochem. 114, 199–227
15 Mitaku, S., Wright, J.K., Best, L. and Jähnig, F. (1984) Biochim. Biophys. Acta 776, 247–258
16 Puskin, J.S. (1977) J. Membrane Biol. 35, 39–55
17 Mekler, V.M., Kotelnikov, A.I., Likhtenstein, G.I. and Berrkovitch, M.A. (1982) Biophysics 27, 403–406
18 Lehrer, S.S. (1971) Biochemistry 10, 3255–3263
19 Shetlar, M.D. (1973) Mol. Photochem., 5, 311–317
20 O'Connor, D.V. and Ware, W.R. (1979) J. Am. Chem. Soc. 101, 121–128
21 Blatt, E., Chatelier, R.C. and Sawyer, W.H. (1984) Photochem. Photobiol. 39, 477–483
22 Fleming, G.R., Knight, A.W.E., Morris, J.M., Morrison, R.J.S. and Robinson, G.W. (1977) J. Am. Chem. Soc. 99, 4306–4311
23 Chapman, D., Williams, R.M. and Ladbrooke, B.D. (1967) Chem. Phys. Lipids 1, 445–475
24 Marsh, D., Watts, A. and Knowles, P.F. (1977) Biochim. Biophys. Acta 465, 500–514
25 Hare, F. (1983) Biophys. J. 42, 205–218
26 Vincent, M., De Foresta, B., Gallay, J. and Alfsen, A. (1982) Biochemistry 21, 708–716
27 Blatt, E., Sawyer, W.H. and Ghiggino, K.P. (1983) Aust. J. Chem. 36, 1079–1086
28 Ghiggino, K.P., Roberts, A.J. and Phillips, D. (1981) Adv. Polymer Sci. 40, 69–167
29 Derzko, Z. and Jacobson, K. (1980) Biochemistry 19, 6050–6057
30 Reers, M., Elbracht, R., Rudel, H. and Spencer, F. (1984) Chem. Phys. Lipids 36, 15–28
31 McLaughlin, S. (1977) in Current Topics in Membranes and Transport (Bonner, F. and Kleinzeller, A., eds.), pp. 71–144, Academic Press, New York
32 Lentz, B.R., Barenholz, Y. and Thompson, T.E. (1976) Biochemistry 15, 4521–4528
33 Chen, L.A., Dale, R.E., Roth, S. and Brand, L. (1977) J. Biol. Chem. 252, 2163–2169
34 Ameloot, M., Hendrickx, H., Herreman, W., Pottel, H., Van Cauwelaert, F. and Van der Meer, W. (1984) Biophys. J. 46, 525–539
35 Marsh, D. (1980) Biochemistry 19, 1632–1637
36 Kinosita, K., Jr., Kawato, S. and Ikegami, A. (1977) Biophys. J. 20, 289–305
37 Heyn, M.P. (1979) FEBS Lett. 108, 359–364
38 Jähnig, F. (1979) Proc. Natl. Acad. Sci. USA 76, 6361–6365
39 Kinosita, K., Jr., Ikegami, A. and Kawato, S. (1982) Biophys. J. 37, 461–464

40 Tanford, C. (1973) in The Hydrophobic Effect, John Wiley & Sons, New York
41 Seelig, J. and Seelig, A. (1980) Q. Rev. Biophys. 13, 19–61
42 Cogan, U., Shinitzky, M., Weber, G. and Nishida, T. (1973) Biochemistry 12, 521–528
43 Matayoshi, E.D., Corin, A.F., Zidovetzki, R., Sawyer, W.H. and Jovin, T.M. (1983) in Mobility and Recognition in Cell Biology (Sund, H. and Veeger, C., eds.), pp. 119–134, Walter de Gruyter, Berlin, New York
44 Corin, A.F., Matayoshi, E.D. and Jovin, T.M. (1985) in Spectroscopy and the Dynamics of Biological Systems (Bayley, P.M. and Dale, R.E., eds.), pp. 53–78, Academic Press, London